Journal of Applied Sciences and Modelling

https://journal.krrishpub.com/index.php/jasm/index

Design and Simulation of an Intelligent Fault Protection Scheme for Smart Grid Applications using Fuzzy Inference and Rate-of-Change Analysis

Tochukwu V. Ikeh [a], Benneth C. Oyinna [a,b,*], Joseph O. Oladele [a]

[a] *Nigerian Electricity Supply Corporation, P.O. Box 15 Bukuru, Jos South, Plateau State, Nigeria.*
[b] *Energy Access and Renewable Energy Technology, Offshore Technology Institute, University of Port Harcourt, Choba, 500102, Nigeria.*

Abstract

With the increasing deployment of smart electrical grids and interoperable digital control infrastructures, intelligent and adaptive fault protection schemes are essential for ensuring system reliability, stability, and rapid fault isolation. This paper presents the design and simulation of an intelligent logic-based fault protection scheme for smart grid applications using fuzzy inference and Rate of Change (RoC) analysis. The proposed system employs a fuzzy logic controller to detect and classify faults by continuously monitoring voltage, current, frequency, and their respective rates of change within an independent electricity distribution network. Unlike traditional protection systems that rely solely on fixed threshold values, the integration of RoC analysis enables faster detection of sudden disturbances, while fuzzy inference provides adaptive, rule-based decision-making under uncertain and dynamic operating conditions. Triangular membership functions are used to evaluate input parameters and generate appropriate protective responses, closely emulating the behavior of modern digital relays. The system is designed to support seamless integration with smart grid communication frameworks, including IEC 61850 protocols, Supervisory Control and Data Acquisition (SCADA), and Generic Object-Oriented Substation Event (GOOSE) messaging. Simulation results obtained using MATLAB/Simulink demonstrate the system's ability to accurately distinguish between normal and fault conditions and to achieve rapid fault isolation with improved sensitivity and reliability. Comparative analysis confirms that the combined fuzzy inference and RoC-based approach significantly enhances protection speed and adaptability compared to conventional methods. The proposed framework provides a scalable and practical solution for intelligent protection in modern smart grid environments and supports potential real-time implementation on embedded and industrial control platforms.

Keywords: MATLAB/Simulink, Fuzzy logic, System protection, Supervisory Control and Data Acquisition (SCADA), Rate of Change (RoC), Smart grid, Power system.

Article information:
DOI: https://doi.org/10.71426/jasm.v1.i1.pp51-59
Received: *25 November 2025* | Revised: *23 December 2025* | Accepted: *29 December 2025*

1. Introduction

Electric power systems represent one of the most critical infrastructures supporting modern economic and societal activities, requiring highly reliable, fast, and selective protection mechanisms to ensure operational continuity and system stability [1], [2]. Under normal operating conditions, electrical currents and voltages remain within predefined limits corresponding to equipment ratings and network design specifications. However, disturbances such as insulation breakdown, lightning strikes, equipment failure, environmental interference, or human activities can introduce faults, resulting in abnormal current flow, voltage collapse, and potential system instability [3], [4]. These fault conditions, if not detected and isolated promptly, may lead to equipment damage, cascading outages, and widespread power system failures.

Fault detection and protection systems play a crucial role in maintaining grid reliability by continuously monitoring system parameters and isolating faulty sections through coordinated relay and circuit breaker operations [5]. Fault severity depends on system impedance, fault location, fault type, and network topology, requiring protection systems capable of accurate and rapid fault identification. Modern smart grid infrastructures further increase protection complexity due to the integration of distributed generation, renewable energy sources, and bidirectional power flow, which introduce dynamic operating conditions and

*Corresponding author
Email address: Ikeh.tochukwu@gmail.com, ikeh.tochukwu@nesconigeria.com (Tochukwu V. Ikeh), bennethoyinna@gmail.com, Benneth.oyinna@nesconigeria.com (Benneth C. Oyinna), josmay2013@gmail.com, Joseph.oladele@nesconigeria.com (Joseph O. Oladele).

uncertainties [3]. These challenges necessitate advanced protection approaches capable of adapting to nonlinear and evolving grid conditions. Traditional protection methods rely primarily on deterministic threshold-based relay logic using over-current, distance, and differential protection principles [2]. While these methods are effective under predictable operating conditions, they exhibit limitations when dealing with nonlinearities, measurement noise, transient disturbances, and complex smart grid configurations [8]. Additionally, detecting high-impedance faults and asymmetrical fault conditions remains particularly challenging using conventional relay techniques due to subtle fault signatures and weak fault currents [6], [12]. These limitations highlight the need for intelligent protection systems capable of adaptive and robust decision-making.

Recent advances in computational intelligence, including artificial neural networks, support vector machines, and fuzzy logic systems, have demonstrated significant potential in improving fault detection and classification accuracy [11]. Among these techniques, fuzzy logic has emerged as a particularly effective approach due to its ability to handle uncertainty, imprecision, and nonlinear system behavior [5]. Unlike conventional binary logic systems, fuzzy logic allows gradual transitions between operating states and incorporates expert knowledge through linguistic rules and membership functions. This capability makes fuzzy logic especially suitable for real-time fault detection and classification in power systems with dynamic and uncertain operating conditions. Fuzzy logic-based protection schemes have been successfully applied to transmission line fault classification, demonstrating improved accuracy and faster response compared to conventional protection methods [7], [10], [13]. Adaptive fuzzy coordination techniques have also been proposed to optimize relay coordination and improve overall system protection performance, particularly in networks with distributed generation and renewable integration [9], [14], [15]. Furthermore, fuzzy logic-based control and protection approaches have been effectively implemented in modern smart grid and renewable energy systems, confirming their suitability for intelligent and decentralized protection applications.

The increasing complexity of modern power systems, particularly in developing countries such as Nigeria, requires intelligent and adaptive protection mechanisms capable of ensuring reliable grid operation. Many developing power systems continue to rely on conventional protection infrastructure, which lacks the flexibility and intelligence required to manage smart grid environments effectively. Integrating intelligent protection systems into these grids can significantly enhance system reliability, reduce fault clearance times, and minimize power outages. This study proposes the design and simulation of a fuzzy logic–based fault protection system for smart grid applications, considering a representative case study in Nigeria. The proposed protection scheme utilizes real-time monitoring of key electrical parameters, including voltage, current, frequency, and rate-of-change signals, to detect and classify faults accurately. The fuzzy logic controller employs a rule-based inference mechanism and membership function modeling to provide fast and selective fault isolation. MATLAB/Simulink and the Fuzzy Logic Toolbox are used to implement and evaluate the proposed protection system under various fault conditions [4]. The performance of the system is analyzed in terms of fault detection speed, selectivity, and reliability. The results demonstrate that the proposed intelligent protection scheme offers significant improvements over conventional protection methods, providing faster fault detection, improved adaptability, and enhanced suitability for modern smart grid environments.

List of symbols and notations.

Symbol	Description and unit
V	Voltage magnitude (V or kV)
I	Current magnitude (A)
f	System frequency (Hz)
$\frac{dV}{dt}$	Rate of change of voltage (V/s)
$\frac{dI}{dt}$	Rate of change of current (A/s)
Z	Transmission line impedance (Ω)
Z_s	Source impedance (Ω)
Z_L	Transmission line impedance (Ω)
I_f	Fault current (A)
t_{trip}	Circuit breaker trip time (s)
R	Transmission line resistance matrix (Ω/km)
Z_{abc}	Phase impedance matrix (Ω/km)
$\mu(x)$	Fuzzy membership function (dimensionless)
FLC	Fuzzy Logic Controller
MF	Membership Function
CB	Circuit Breaker
3LG	Three-phase to ground fault
DLG	Double line-to-ground fault
SLG	Single line-to-ground fault
RoC	Rate of Change
VT	Voltage Transformer
CT	Current Transformer

2. Methodology

2.1. System overview

The proposed system monitors three primary parameters: voltage, current, and frequency at two selected buses in the power system. The first bus is modeled as the line input of a main feeder, while the second bus is modelled as a tee-off from the first line. These input signals are continuously assessed to determine whether they remain within acceptable operating ranges. The fuzzy logic controller evaluates the absolute values of these signals to detect anomalies indicative of faults. A high-level block diagram of the proposed system is shown in Figure 1. The 33 kV power source was modeled as a generator connected to an infinite bus for both steady-state and dynamic analyses. The transmission line was modeled using the parameters of an ACSR "Panther" conductor to achieve realistic.

2.2. Input signal acquisition and pre-processing

The method adopted for voltage monitoring involves a voltage transformer (VT) that steps down 33 kV to 12 V. The 12 V signal is then fed into the fuzzy logic controller (FLC), which, based on its programmed rules, sends a *trip* signal whenever the voltage falls outside predefined thresholds. An indication signal is also generated to indicate over-voltage or under-voltage conditions.

For current monitoring, current transformers (CTs) were used to step down the line current from 200 A to 5 A for both line-1 and line-2. These CTs are typically integrated within circuit breakers and are flux-dependent, measuring current based on Faraday's law. The 5 A output is used by the FLC to generate trip and indication signals whenever current exceeds the preset limits.

Frequency monitoring is implemented using an operational amplifier (op-amp) based zero-crossing detector and a timer. The measured frequency is sent to the FLC, which triggers the breaker and provides an indication whenever the frequency is outside acceptable limits.

Additionally, the RoC of voltage and current is considered, measuring how quickly these parameters increase or decrease over time, allowing faster fault detection. In real-time implementations, the voltage, current, and frequency signals are obtained either from simulation blocks or physical sensors, and are normalized for fuzzy logic processing.

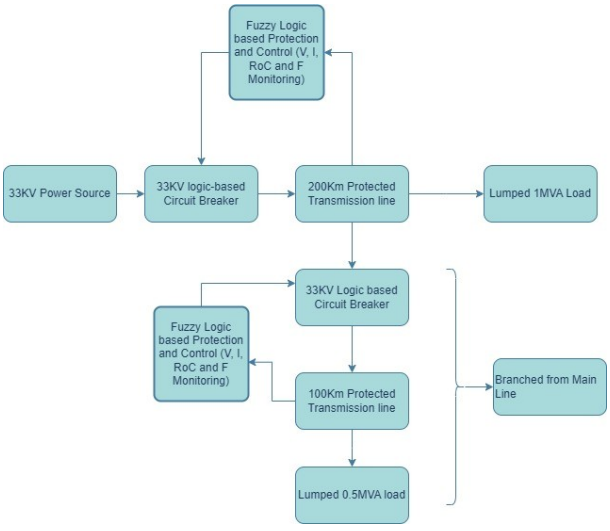

Figure 1: High-level block diagram of the proposed system.

Hence, for each parameter, two input sets are generated:

- Absolute Magnitude (e.g., current magnitude)
- Rate of Change (e.g., dI/dt, dV/dt)

2.3. Fuzzification

Each input is converted into fuzzy variables using membership functions (triangular and trapezoidal). The fuzzy sets are defined as follows:

- Voltage: Under-voltage, Normal, Over-voltage
- Current: Normal, High
- Frequency: Low, Normal, High
- Rate of Change (for I and V): Negative, Zero, Positive

Membership functions are designed with smooth overlap to allow gradual transitions between fuzzy states, improving detection sensitivity. Figure 2 illustrates the membership functions for current magnitude and RoC.

2.4. Rule-base design

A total of 39 fuzzy rules were designed based on expert knowledge of power system fault behavior. The rules cover combinations of abnormal voltage, over-current, frequency deviations, and sudden transients.

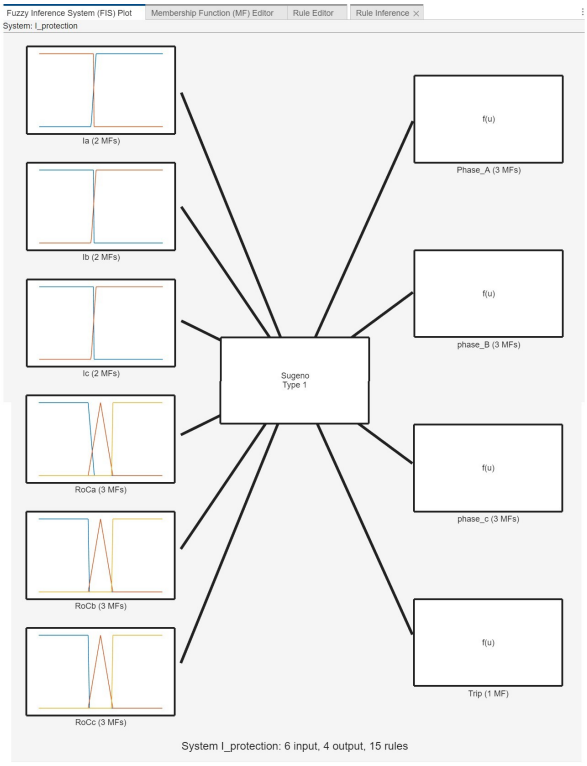

Figure 2: Membership functions for current magnitude and RoC.

2.5. Fault classification and action logic

The defuzzified output drives a decision-making block that performs:

- Display of status (*Over-current*, *Over-voltage*, *Over-frequency*, *Load loss*)
- Protection logic (breaker trip)

Figure 3 shows the MATLAB/Simulink implementation of the fuzzy logic-based fault detection system.

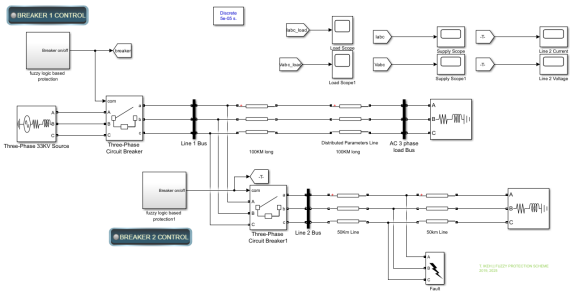

Figure 3: MATLAB/Simulink model of the fuzzy logic-based fault detection system.

2.6. System testing and valuation

The system was tested under a line-to-line-to-line-to-ground (L-L-L-G) fault, applied 50 km along Line 2. The breaker on line-2 is expected to trip while maintaining supply to line-1.

3. Design calculations

This section presents the analytical design and protection calculations for the developed transmission line protection system. The analysis includes normal load current estimation, fault current derivation using impedance modelling, sequence impedance formulation, and rate-of-change based protection criteria. The equations and tabulated values form the quantitative basis for relay setting and system validation.

3.1. Normal load currents

This subsection establishes the baseline operating current levels of the protected transmission lines. These currents determine relay pickup thresholds and protection sensitivity. For Line 1, the normal load current is written as (1).

$$I_{L1} = 60 \text{ A} \tag{1}$$

After the current transformer scaling, the relay-side current becomes (2):

$$I_{L1,CT} = \frac{I_{L1}}{\text{CTR}} = 1.5 \text{ A} \tag{2}$$

Similarly, the normal load current for line 2 is written as (3):

$$I_{L2} = 20 \text{ A} \tag{3}$$

and after CT scaling becomes (4).

$$I_{L2,CT} = 0.5 \text{ A} \tag{4}$$

Equations (1)–(4) define the steady-state operating region and form the reference point for detecting abnormal conditions such as faults or overloads.

3.2. Fault current calculation

This subsection derives the general expression for fault current based on equivalent circuit modelling. The fault current is given by (5).

$$I_f = \frac{V_{ph}}{Z_s + Z_L + Z_f} \tag{5}$$

In (5),

$$V_{ph} = \frac{V_{LL}}{\sqrt{3}} \tag{6}$$

For a bolted fault, the fault impedance value is (7).

$$Z_f \approx 0 \tag{7}$$

Thus, fault current becomes inversely proportional to total system impedance as seen from the fault point, as evident from (5).

The source impedance is defined as (9).

$$Z_s = R + jX \tag{8}$$

Substituting the given values in (8), then:

$$Z_s = 0.8929 + j0.01658 \tag{9}$$

Magnitude value is calculated in (10).

$$|Z_s| = \sqrt{(0.8929)^2 + (0.01658)^2} = 0.8931 \ \Omega \tag{10}$$

The (10) represents the Thevenin equivalent impedance of the upstream power system.

3.3. Line parameters

This subsection defines the electrical parameters of the transmission line using distributed parameter modelling.

The resistance matrix is written as (11) and the Equation (11) represents conductor resistance including mutual coupling.

$$R = \begin{bmatrix} 0.058637 & 0.056285 & 0.056232 \\ 0.056285 & 0.058639 & 0.056285 \\ 0.056232 & 0.056285 & 0.058637 \end{bmatrix} \ \Omega/\text{km} \tag{11}$$

The inductance matrix is given by (12) and the Equation (12) defines energy storage characteristics of the line.

$$L = \begin{bmatrix} 1.5962 \times 10^{-3} & 8.4773 \times 10^{-4} & 7.0927 \times 10^{-4} \\ 8.4773 \times 10^{-4} & 1.5962 \times 10^{-3} & 8.4773 \times 10^{-4} \\ 7.0927 \times 10^{-4} & 8.4773 \times 10^{-4} & 1.5962 \times 10^{-3} \end{bmatrix} \ \text{H/km} \tag{12}$$

The admittance matrix is given by (13) and the impedance matrix is derived as (14). Further, the equation (14) forms the basis for the calculation of the sequence impedance.

$$Y = \begin{bmatrix} 3.82 \times 10^{-6} & -8.82 \times 10^{-7} & -2.83 \times 10^{-7} \\ -8.82 \times 10^{-7} & 4.00 \times 10^{-6} & -8.82 \times 10^{-7} \\ -2.83 \times 10^{-7} & -8.82 \times 10^{-7} & 3.82 \times 10^{-6} \end{bmatrix} \ \text{S/km} \tag{13}$$

$$Z_{abc} = \begin{bmatrix} 0.5049 & 0.2722 & 0.2295 \\ 0.2722 & 0.5049 & 0.2722 \\ 0.2295 & 0.2722 & 0.5049 \end{bmatrix} \ \Omega/\text{km} \tag{14}$$

3.4. Sequence impedance

This subsection converts phase impedance to sequence impedance using the symmetrical component transformation (15)-(17) and the resulting values are (18)-(19). The impedance values obtained determine the magnitude of fault current depending on fault type.

$$Z_0 = Z_s + 2Z_m \tag{15}$$

$$Z_1 = Z_s - Z_m \tag{16}$$

$$Z_2 = Z_1 \tag{17}$$

$$Z_0 = 1.0209 \ \Omega/\text{km} \tag{18}$$

$$Z_1 = Z_2 = 0.2469 \ \Omega/\text{km} \tag{19}$$

Table 1: Fault current for SLG.

Fault location	Z_{tot} **(Ω)**	I_f **(A)**
1 km	2.407	16,713.26
50 km	76.628	248.64
100 km	152.363	121.85
200 km	303.833	62.71

Note: $Z_{\text{tot}} = Z_s + (1.5147 \times d)$, where d is the fault distance in km.

Table 2: Fault current for DLG.

Fault location	Z_{tot} **(Ω)**	I_f **(A)**
1 km	1.225	15,542.05
50 km	17.533	1,086.68
100 km	34.173	557.54
200 km	67.453	282.46

Note: $Z_{\text{tot}} = Z_s + (0.3328 \times d)$, where d is the fault distance in km.

3.5. Fault current calculations

This subsection evaluates the magnitude of fault currents at different locations along the transmission line under various fault conditions. The fault current is calculated using Equation (5), which shows that the fault current magnitude is inversely proportional to the total impedance between the source and the fault point. As the distance from the source increases, the line impedance increases proportionally, thereby reducing the fault current magnitude.

In this work, the SLG, DLG, and 3-LG faults were analyzed to evaluate the protection system performance under different fault scenarios. The calculated results provide insight into how impedance variation affects fault severity and protection response.

Table 1 presents the calculated SLG fault currents at various distances along the transmission line. It is observed that the fault current decreases significantly with increasing distance. At a fault location of 1 km, the fault current reaches a maximum value of 16,713.26 A due to the relatively low total impedance. However, at 200 km, the fault current reduces to 62.71 A as the impedance increases substantially. This reduction demonstrates the direct impact of line impedance on limiting fault current magnitude. Similarly, Table 2 shows the calculated fault current values for DLG faults. Compared to SLG faults, DLG faults exhibit slightly lower impedance and therefore produce relatively higher fault currents at comparable distances. At 1 km, the fault current reaches 15,542.05 A, while at 200 km, the fault current decreases to 282.46 A. This trend confirms that line impedance plays a dominant role in determining the magnitude of fault current and the effectiveness of protection schemes. Table 3 presents the calculated fault current values for three-phase-to-ground faults, which represent the most severe fault condition in power systems. It is observed that the fault current is highest at locations closer to the source and gradually decreases as the fault distance increases. For example, the fault current at 1 km is 16,713.26 A, while at 200 km it reduces to 378.99 A. This behavior confirms that increasing transmission line impedance limits fault current magnitude and improves system stability.

Table 3: Fault current calculations for three-phase-to-ground fault.

Fault location	$Z_s + Z_L$ **(Ω)**	I_f **(A)**
1 km	1.14	16713.26
50 km	13.2381	1439.25
100 km	25.5831	744.75
200 km	50.2731	378.99

From Tables 1, 2, and 3, it is evident that the fault current magnitude decreases with increasing fault distance due to the rise in total system impedance. These results validate the theoretical fault current model described in Equation (5) and confirm the effectiveness of the proposed protection system in detecting faults under different operating conditions. The calculated fault current values provide essential input parameters for configuring protection thresholds, fuzzy logic rules, and circuit breaker coordination in the proposed smart grid protection framework.

3.6. Rate of change protection

This subsection defines protection logic based on current variation rate. The RoC is defined as (20).

$$RoC = \frac{\Delta I}{\Delta t} \tag{20}$$

The obtained value of RoC of line-1 and line-2 RoC are (21) and (22), respectively and these values define relay tripping thresholds.

$$RoC_1 = \frac{0.75}{500 \times 10^{-6}} = 1500 \tag{21}$$

$$RoC_2 = \frac{0.25}{500 \times 10^{-6}} = 500 \tag{22}$$

3.7. Voltage protection

The Minimum and maximum limits of the voltage protection are defined as (23) and (24), respectively.

$$V_{min} = 0.94 \times 33 = 31.02 \text{ kV} \tag{23}$$

$$V_{max} = 1.06 \times 33 = 34.98 \text{ kV} \tag{24}$$

The RoC voltage is written as (25) and it defines the voltage protection threshold.

$$RoC_V = \frac{12 - 11.28}{500 \times 10^{-6}} = 1440 \text{ V/s} \tag{25}$$

4. Results and discussion

4.1. MATLAB/Simulation based results

The proposed fuzzy logic-based fault detection and isolation scheme was implemented in MATLAB/Simulink using a two-bus transmission system with a tee-off branch, as shown in the simulation model. Faults were introduced on the remote tee-off line to evaluate the performance, speed, and selectivity of the protection scheme.

The fuzzy logic controller continuously monitored system parameters including voltage magnitude, current magnitude, frequency magnitude, rate of change of voltage

(RoC-V), and rate of change of current (RoC-I). These parameters enabled rapid detection of abnormal operating conditions and ensured fast isolation of faulty sections.

The simulation results corresponding to various fault conditions are presented in Figures 4–15. The fault was applied at the midpoint of the tee-off transmission line (50 km from the bus) at $t = 0.7$ s.

4.1.1. Under 3-LG fault condition

An L-L-L-G fault was applied at $t = 0.7$ s to analyze the system response under severe fault conditions. Figure 4 shows the line-2 voltage waveform under the 3-LG fault condition. Prior to fault occurrence, the voltage remains stable at its nominal value, confirming normal steady-state operation. Immediately after the fault initiation, the voltage collapses sharply due to the short-circuit condition and reaches zero after breaker operation, demonstrating effective fault detection and isolation.

The transient oscillations visible in Figure 4 also confirm the electromagnetic response of the system during the fault initiation and clearing, validating the sensitivity of voltage magnitude as a reliable fault detection parameter.

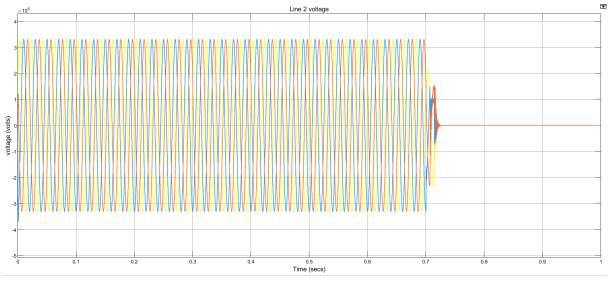

Figure 4: Line-2 voltage under 3-LG fault.

Figure 5 illustrates the current waveform during the 3-LG fault condition. The current magnitude increases rapidly to approximately 1600 A immediately after the fault due to reduced fault impedance. This confirms the severe nature of the three-phase fault.

After breaker isolation, the current drops to zero, indicating complete fault clearance. Additionally, the healthy feeder remains unaffected, confirms the selectivity of the fuzzy logic protection system.

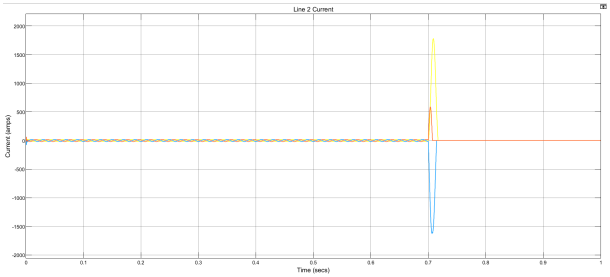

Figure 5: Current waveform showing line isolation under 3-LG fault.

Figure 6 shows the circuit breaker control signal. The breaker remains in the closed state (logic 1) under normal conditions and transitions to open state (logic 0) after fault detection.

This confirms that the fuzzy logic controller successfully detects the fault and generates the appropriate trip command without delay.

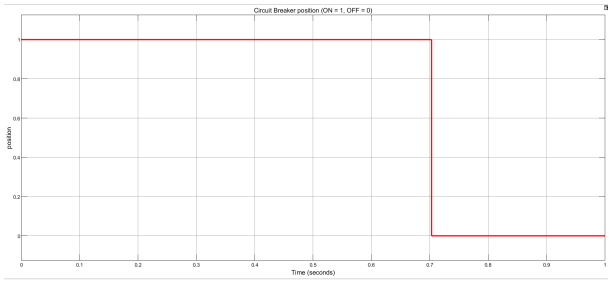

Figure 6: Circuit breaker open/close pulses

Figure 7 provides a zoomed view of breaker operation, clearly showing that the breaker opens at $t = 0.703$ s. This corresponds to a trip delay of approximately 3 ms after fault initiation.

This fast response demonstrates the high-speed detection capability of the fuzzy logic protection scheme.

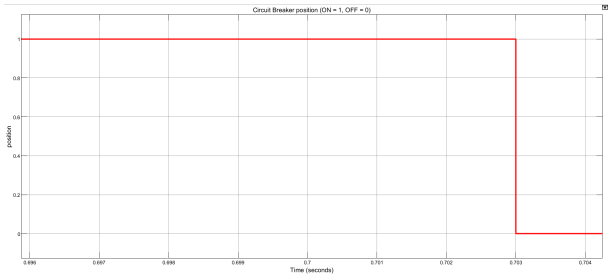

Figure 7: Circuit breaker trip control showing 3 ms delay.

4.1.2. Measurement Outputs

The measurement scaling provided by current transformers and voltage transformers is summarized in Table 4. These transformers safely convert high-voltage and high-current signals into measurable low-voltage signals suitable for control and protection systems.

The scaling ensures accurate signal representation while maintaining electrical isolation and system safety.

Table 4: CT outputs and voltage outputs.

Measuring point	Rating	HV Side	Output
Grid supply voltage	33,000/12 V	33 kV	12 V
Line-1 supply current	200/5 A	60 A	1.5 A
Line-2 supply current	200/5 A	20 A	0.5 A

4.1.3. ROC Signals

Figure 8 shows the RoC of voltage during the 3-LG fault condition. A sharp spike is observed at the fault instant ($t = 0.7$ s), clearly distinguishing fault conditions from normal operation.

This confirms that the RoC of voltage is an effective and sensitive parameter for rapid fault detection.

Similarly, Figure 9 shows the RoC of current during fault initiation. The RoC signal exhibits large transient spikes, providing a reliable indication of sudden abnormal current variation. Following breaker isolation, the RoC signal stabilizes, confirming successful fault clearance.

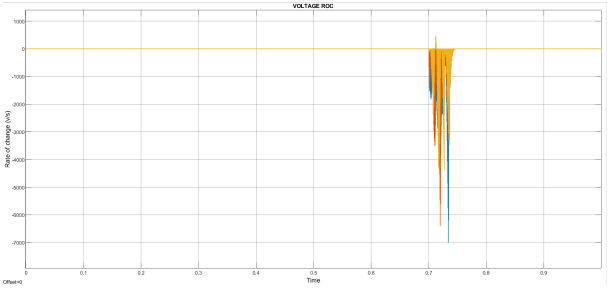

Figure 8: RoC of voltage under 3-LG fault.

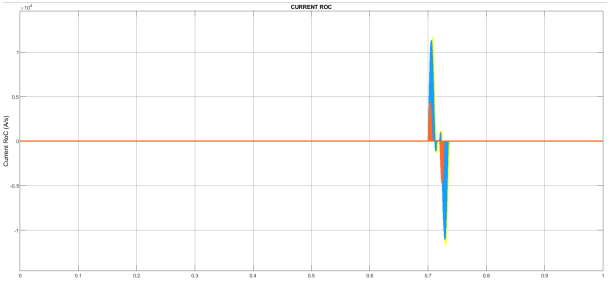

Figure 9: RoC of current under 3-LG fault.

4.1.4. DLG Fault

Figure 10 shows the line-2 current under double-line-to-ground fault conditions. The current magnitude increases significantly, confirming fault occurrence. However, the magnitude is lower compared to the 3-LG fault due to asymmetrical fault conditions.

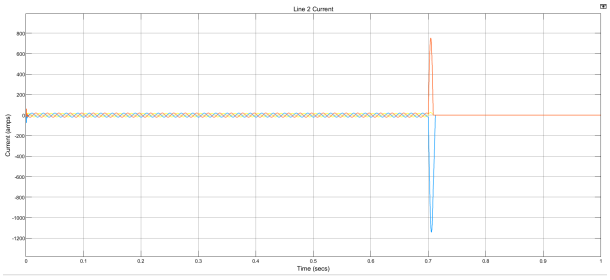

Figure 10: Line-2 current under DLG fault.

The RoC of current shown in Figure 11 clearly exhibits transient spikes during the fault condition, enabling rapid detection by the fuzzy controller.

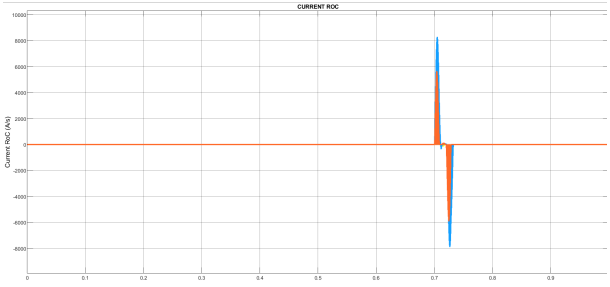

Figure 11: RoC of current under DLG fault.

The breaker operation under DLG fault is shown in Figure 12. The breaker successfully isolates the fault within approximately 3 ms.

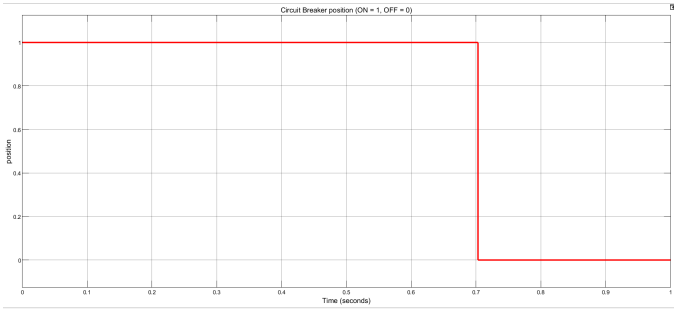

Figure 12: Breaker position under DLG fault.

4.1.5. SLG Fault

Figure 13 shows the line-2 current under SLG fault conditions. The fault current magnitude is lower compared to other fault types due to higher fault impedance.

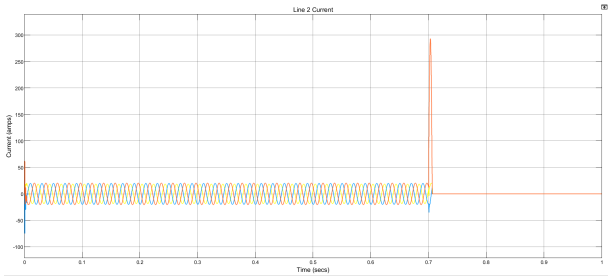

Figure 13: Line-2 current under SLG fault.

The RoC of current shown in Figure 14 clearly detects the transient fault condition, confirming the sensitivity of the fuzzy protection scheme.

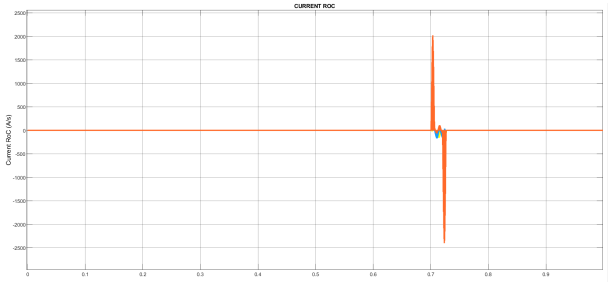

Figure 14: RoC of Current under SLG fault.

Breaker operation under SLG fault is shown in Figure 15. The breaker isolates the fault successfully within 5.5 ms.

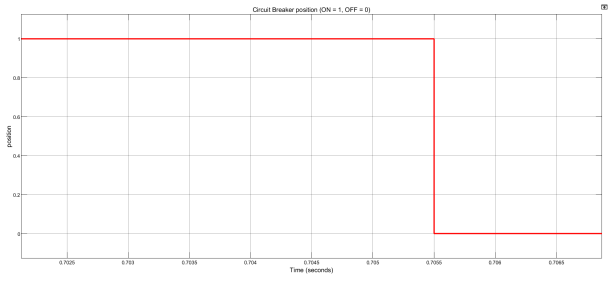

Figure 15: Breaker position under SLG fault.

4.1.6. Summary of results

The overall protection performance is summarized in Table 5. The results show extremely fast fault detection and isolation across all fault types.

Table 5: Result summary of trip times.

Fault type	**Fault current (A)**	**Trip time (s)**
3LG	1600	0.003
DLG	1100	0.003
SLG	290	0.0055

The fuzzy protection system provides fast, selective, and reliable protection with trip times between 3 ms and 5.5 ms.

4.2. Discussions

The results obtained show that the simulated model adequately and efficiently protected the modelled system against faults along the line.

During normal operation, the protection scheme constantly checks the system parameters (voltage, current and frequency) for any abnormal value which arises as a result of fault along the line. When an abnormality is detected, the supply is isolated from the load to protect the system from damage. The simulation results show that the scheme does not negatively affect the operation of the system during normal condition as the phase sequence and other necessary parameters were all seen to be unaffected.

The scheme utilized also utilized the rate of change of these parameters, which was able to ensure faster switching and isolation of the faulty sections. This was achieved in max of 5.5 milliseconds in this simulation as opposed to 0.5 to 2 secs normally achieved in traditional relays. Additionally, relay coordination and selectivity was achieved as the faulty section of the line was isolated and the healthy part was still left in circuit with no interruptions (minor voltage dips was seen on the healthy side prior to the isolation).

When a permanent or transient fault was introduced into the system, the results showed that the protection scheme immediately came into action detecting the exact fault and sending the trip pulse to the circuit breaker to open and isolate the supply. The results showed that the protection had the fastest detection time for more severe faults and a detection time of 5.5 milliseconds for SLG faults before sending the trip pulse to the CB. However, this delay is so small and is acceptable for power system protection as the time of operation only allows a period (1/50) of the fault current to pass hence the load does not even experience the fault current as seen in the simulation results.

This fast action is attributed to the addition of the rate of change parameter which detects and cuts off the faulty section quickly. A major disadvantage however is the use of the stabilizing delay to delay fault detection when the line is just energized. As a result, a fault on the line at the first point of closure will not be selected by the rate of change parameter but will be detected by the over-current relay.

To show the performance of a fault present on the line at point of closure, a 3-phase-to-ground fault is made to appear on the line-2 from the start of the simulation. Due to the use of a stabilizing relay for the rate of change, the RoC checks will therefore be inactive, however the over-current, over/under voltage and over-frequency checks will still be active.

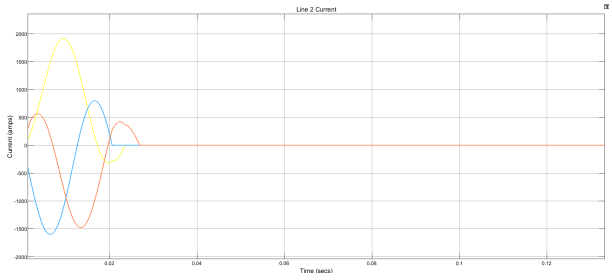

Figure 16: Line-2 current with 3-LG fault active from feeder closure.

Figure 16 shows that the over-current still tripped the breaker after 0.02 secs (20 milliseconds). This is opposed to trip time of 3 milliseconds achieved with the RoC checks. The breaker position is shown below.

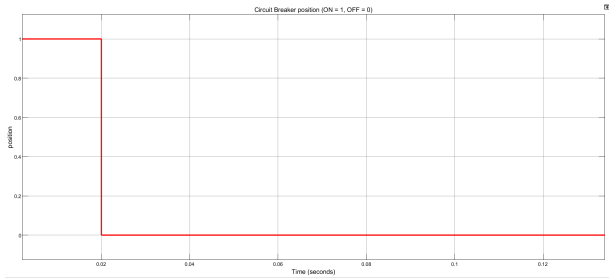

Figure 17: Breaker position with RoC suspended.

The breaker is seen to only get the trip signal after 20 milliseconds as the RoC checks are suspended at breaker closure shown in Figure 17.

A trip time of 20 milliseconds is faster than traditional relay trip times of 0.5 to 2 secs but the results show that using the RoC parameter, properly tuned to pick up all faults can significantly reduce the response time of relays and ensure faster trip times as low as 5 milliseconds.

The fast operation of the protection to trip the CB under fault conditions shows that using fuzzy logic programming for protection purposes is a suitable and fast-acting method of system protection. Also, the supply to the load is not affected by the protection scheme and very little power is consumed in the scheme itself due to the fact it utilizes mostly logic inputs and outputs. Electromechanical protection techniques used in Nigerian power system today consumes some form of the power to operate its relays and also there is the cost of these coils and relays. The scheme used in this work on the other hand, is seen to be relatively cheap as it uses cheaper electronic components and ICs, it has little moving parts as programming controls most of its operation which reduces the maintenance requirements on them. Also, since the protection scheme is programmed into the controller, it makes the scheme more adaptable as just a little change in program would suffice as opposed to having to change the entire components of protection when the new system is at a different voltage, frequency or current value.

5. Conclusion

Fuzzy logic detection serves better in the electric power grid setup, especially when rate-of-change and other input features are added, as compared to the conventional

threshold setting detection methods. Since distributed energy resources, electric vehicles, and renewable energy sources increasingly become part of the mix, multifarious decision-making, uncertainty, and fluctuation come into play; it, therefore, finds good use in SCADA and smart grid applications. Fuzzy logic finds application in fault detection, voltage and frequency control, load forecasting, and renewable energy integration. It smoothens the impact of erratic load with predictions regarding short- and long-term loads, infusion of weather data, and consumption patterns, different from what the statistical models perform. Also, enhancements could comprise hardware implementation, multi-bus scalability, adaptive rule tuning, AI intelligent methods for dynamic rule updates, and testing with embedded devices for real-time protection.

Declarations and Ethical Statements

Conflict of Interest: The author declare that there is no conflict of interest.

Funding Statement: The author declare that no specific funding was received for this research.

Artificial Intelligence usage Statement: During the preparation of this manuscript, the author utilized ChatGPT solely for language refinement and grammatical corrections. The author carefully reviewed and revised the generated content and take full responsibility for the accuracy, integrity, and originality of the final manuscript.

Availability of Data and Materials: The data and/or materials that support the findings of this study are available from the corresponding author upon reasonable request.

Publisher's Note: The publisher of this article, Krrish Scientific Publications, remains neutral with regard to jurisdictional claims in published maps and institutional affiliations.

References

[1] Glover JD, Sarma MS, Overbye TJ, Padhy NP. Power system analysis and design. 5th ed. Stamford, CT, USA: Cengage Learning; 2012.

[2] IEEE Power System Relaying Committee. IEEE guide for protective relay applications to power system buses. *IEEE Std C37.234-2009*; 2009. Available from: https://doi.org/10.1109/IEEESTD.2009.5325912

[3] Dehghanpour K, Wang Z, Wang J, Yuan Y, Bu F. A survey on state estimation techniques and challenges in smart distribution systems. *IEEE Transactions on Smart Grid*. 2018 Sep 17;10(2):2312–22. Available from: https://doi.org/10.1109/tsg.2018.2870600

[4] [Online Available]: Fuzzy Logic Toolbox Release Notes. *MathWorks*. Available from: https://www.mathworks.com/help/fuzzy/release-notes.html

[5] Zadeh LA. Fuzzy sets. *Information and Control*. 1965;8(3):338–353. Available from: https://doi.org/10.1016/S0019-9958(65)90241-X

[6] Mathew R, Aneesh VA. High Impedance Fault Detection using Wavelet Transform and Artificial Neural Network. *AIJR Proceedings*. 2023 Dec 22;403–10. Available from: http://dx.doi.org/10.21467/proceedings.160.52

[7] Mahanty RN, Gupta PBD. A fuzzy logic based fault classification approach using current samples only. *Electric Power Systems Research*. 2006 Jun 11;77(5–6):501–7. Available from: https://doi.org/10.1016/j.epsr.2006.04.009

[8] Dutta P, Esmaeilian A, Kezunovic M. Transmission-Line fault analysis using synchronized sampling. *IEEE Transactions on Power Delivery*. 2014 Feb 19;29(2):942–50. Available from: https://doi.org/10.1109/tpwrd.2013.2296788

[9] Sampaio FC, Tofoli FL, Melo LS, Barroso GC, Sampaio RF, Leão RPS. Adaptive fuzzy directional bat algorithm for the optimal coordination of protection systems based on directional overcurrent relays. *Electric Power Systems Research*. 2022 Jul 15;211:108619. Available from: https://doi.org/10.1016/j.epsr.2022.108619

[10] Kumar P, Jamil M, Thomas MS. Fuzzy approach to fault classification for transmission line protection. In *Proceedings of IEEE. IEEE Region 10 Conference. TENCON 99.'Multimedia Technology for Asia-Pacific Information Infrastructure'(Cat. No. 99CH37030)* 1999 Sep 15 (Vol. 2, pp. 1046-1050). IEEE. Available from: https://ieeexplore.ieee.org/document/818602

[11] Dash PK, Samantaray SR, Panda G. Fault Classification and Section Identification of an Advanced Series-Compensated Transmission Line Using Support Vector Machine. *IEEE Transactions on Power Delivery*. 2007 Jan 1;22(1):67–73. Available from: https://doi.org/10.1109/tpwrd.2006.876695

[12] Sekar K, Mohanty NK. High impedance fault detection in distribution system. *International Journal of Advances in Applied Sciences*. 2019 Jun 1;8(2):95. Available from: https://doi.org/10.11591/ijaas.v8.i2.pp95-102

[13] Taheri M, Parhamfar M, Hajarkesht A, Soleimani A, Güven AF. A systematic approach for protective relay coordination and transient stability examination in energy networks with substantial DG. *Journal of Modern Technology*. 2025;2(1):264–282. Available from: https://doi.org/10.71426/jmt.v2.i1.pp264-282

[14] Pidikiti T, Gireesha B, Subbarao M, Krishna VM. Design and control of Takagi-Sugeno-Kang fuzzy based inverter for power quality improvement in grid-tied PV systems. *Measurement: Sensors*. 2023 Feb 1;25:100638.Available from: https://doi.org/10.1016/j.measen.2022.100638

[15] Kumar GN, Sai RV, Reddy TM, Shajid SK, Boora K. Emulation of wind turbine system using fuzzy controller-based vector controlled induction motor drive. *Journal of Modern Technology*. 2024 Sep 8:38-46. Available from: https://doi.org/10.71426/jmt.v1.i1.pp3-46